Optical design of the ultra-light-weight FIRST telescope

E. J. Cohen[a*], A. B. Hull[a], J. Escobedo-Torres[b], D. D. Barber[c], R. A. Johnston[c], D. W. Small[c], A. Prata, Jr.[d], and E. R. Freniere[e]

[a]Jet Propulsion Laboratory, California Institute of Technology, 4800 Oak Grove Drive, Pasadena, California 91109-8099
[b]Composite Optics, Inc., 9617 Distribution Ave., San Diego California 92121
[c]LightWorks Optics, Incorporated, 2691 Richter Ave., Suite 105, Irvine, CA 92606
[d]University of Southern California, Los Angeles, California 90089-0271
[e]Lambda Research Corporation, 80 Taylor Street, Littleton, Massachusetts 01460-4400

ABSTRACT

The FIRST telescope will be made of carbon fiber reinforced plastic. The optics follow a two mirror near-classical Ritchey-Chretian design, but deviates from that in two respects. The secondary mirror defines the pupil of the system, and the primary mirror is uncommonly fast at f/0.5. After presenting the optical design, the sensitivities will be presented.

Current work in progress will be described in the following areas;
1 - secondary mirror figure correction
2 - stray light
3 - primary mirror gaps
4 - standing wave impact on the heterodyne instrument for FIRST (HIFI).

Keywords: FIRST, telescope, far-infrared, primary mirror, secondary mirror, Ritchey-Chretian, Cassegrain, telescope sensitivities, stray light, standing waves

1. INTRODUCTION

The Far Infrared and Submillimeter Telescope (FIRST) telescope has been described in other papers at this conference[1,2] and is shown in figure 1. FIRST is an ESA mission scheduled for launch in 2007. NASA is a junior partner on this mission and has asked the Jet Propulsion Laboratory (JPL) to deliver the FIRST telescope to ESTEC. JPL is working with Composite Optics, Incorporated (COI), who is designing and fabricating the telescope, and with LightWorks Optics, who is designing the optics.

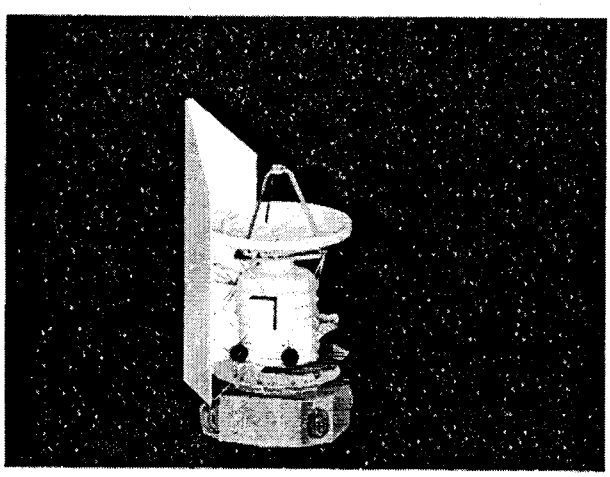

Figure 1. FIRST Telescope

* Correspondence: Email: Eri.J.Cohen@jpl.nasa.gov; Telephone: 818-354-0086; FAX: 818-393-6869

Optical requirements for the telescope are driven by the need to be diffraction limited at 80 μm. The most important optical requirements that characterize the telescope are listed in table 1.

Table 1. Optical Requirements for the FIRST Telescope

Bandwidth	80 - 670 μm
Telescope wavefront error (WFE)	≤10 μm rms., ≤6 μm rms. goal
Diameter	3,500 mm
Focal Length of primary	1,750 mm
System focal length	28,500 mm
System f number	8.68
Diameter of effective aperture	3,280.2 mm
Field of view (FOV)	± 0.25°
Aperture stop	Secondary mirror
Surface roughness	≤0.6 μm rms.
Relative spectral transmission	≥97% at delivery of telescope

ESTEC requires the telescope design to be a 2 mirror telescope, either a Cassegrain or a Ritchey-Chretian. We have chosen the latter. The reasoning is that the performance of the system can be improved by making the primary slightly hyperbolic and compensating for this change by increasing the eccentricity of the secondary to produce a perfect image on axis. With the proper choice of eccentricities for the primary and secondary, both the spherical aberration and the coma can be corrected, leaving astigmatism and field curvature uncorrected. This system configuration is called a Ritchey-Chretian.

Three focal plane instruments are fed by the telescope with an f/8.68 beam. All instruments are cryogenically cooled and share the focal plane. The HIFI[3] instrument is strictly a spectrometer while the photoconductor array camera and spectrometer (PACS)[4] and the spectral and photometric imaging receiver (SPIRE)[5] are both spectrometers and imaging photometers. Figure 2 shows how the instruments split up the focal plane and table 2 summarizes key instrument characteristics.

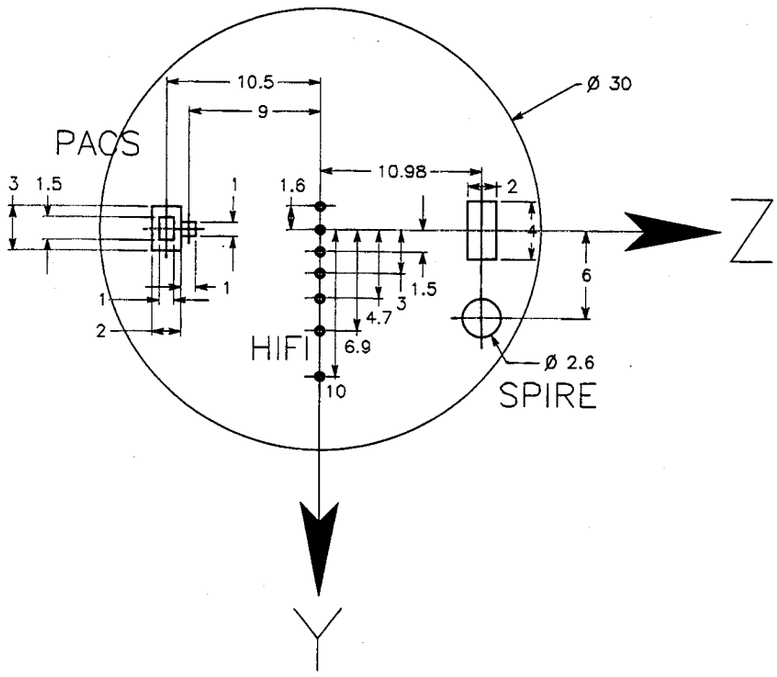

Figure 2. Position of Instruments in Focal Plane in Terms of Field Angle (units are in arcminutes)

Table 2. FIRST Instrument Characteristics That Relate to the Telescope

Instrument	Bandwidth	Field of view	Off -axis location
PACS			
Imager	80 - 130 μm	1'x1.5'	z ~ +10.5'
Imager	130 - 210 μm	2'x3'	z ~ +10.5'
Spectrometer	80 - 110 μm 110 - 210 μm	1'x1'	z ~ +9'
SPIRE			
Imager	3 bands centered at 250, 350 and 500 μm each with $\lambda/\Delta\lambda = 3$	2'x4'	z = -10.98'
Spectrometer	200 - 300 μm 300 - 670 μm	2.6' diameter	z = -10.98 y ~ -6'
HIFI			
Channel 1	467 - 625 μm		y = -10.0'
Channel 2	374 - 469 μm		y = -6.9'
Channel 3	311 - 375 μm		y = -4.7'
Channel 4	267 - 312 μm		y = -3.0'
Channel 5	240 - 268 μm		y = -1.5'
Channel 6	157 - 213 μm		y = 0
Channel 7	111 - 125 μm		y = +1.6'

The 6 μm rms goal is driven by the diffraction limited performance for the PACS instrument, which observes at the shortest wavelength (80 μm) of all the instruments. Both the SPIRE and PACS instruments are background noise limited by the telescope's thermal noise and therefore require extremely low emissivity from all surfaces in view of the detectors. In order to keep a nearly constant thermal background when chopping, PACS and SPIRE chop along a primary mirror isotherm. Thus they both chop about the z-axis, SPIRE by ±2' and PACS by ±3'. HIFI is not background noise limited and chops by ±1.5' about the y-axis.

2. OPTICAL DESIGN

With the distance from the vertex of the primary mirror to the best axial focus of the system specified to be 1,050.162 mm, the system is completely defined. The radius of curvature (ROC), diameter, and conic constants of the 3 surfaces are presented in table 3.

Table 3. Optical Prescription

Surface	ROC (mm)	Diameter (mm)	Conic constant	Optical curvature depth (mm)
Primary mirror	3,500	3,465.361†	-1.00129	437.465*
Secondary mirror	345.264	308.3000	-1.29600	33.919
Focal surface	167.171	244.9497	-1	44.865

† Diameter of the primary needed to cover the full FOV of the telescope.

* Optical curvature depth for primary is based on a diameter of 3,500 mm.

Figure 3 shows all the surfaces described in table 3. Another useful parameter is the secondary magnification, which is 16.286.

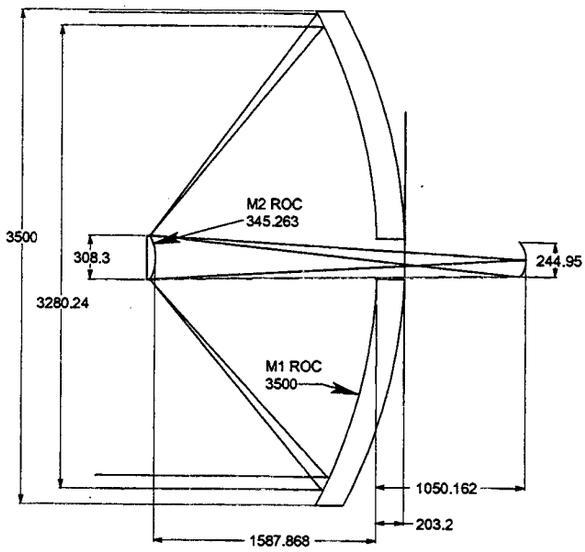

Figure 3. Optical Surfaces and Their Dimensions (all units in mm)

Since the secondary is the pupil of the system, the footprint of the secondary on the primary depends on the field angle observed. To prevent vignetting the diameter of the primary mirror must be at least 3,466 mm, which is the same as saying that for all field angles within the FOV (±15'), the aperture beyond the 3,466 mm diameter is not used. Due to diffraction, the detectors will see beyond this diameter but by looking at the outer rim of the primary, instead of the region off the edge of the primary, which might be warm, the detectors will see cold sky. The maximum diameter of the primary that avoids vignetting should be compared to the effective on-axis aperture diameter of 3,280.2 mm. The movement of the edge of the footprint of the secondary on the primary is roughly 6.35 mm/arcmin near the center of the field and 6.72 mm/arcmin near the edge of the field.

The hole in the primary has a minimum and maximum range. All rays from the secondary to focal surface, for all positions on the focal surface, require a hole in the primary of a minimum diameter of 269 mm for clearance of all rays. The maximum size of the hole is determined by following all plane waves for the full FOV. To make sure that all rays, that are not obscured by the secondary, do not pass directly through the hole in the primary, but are reflected to the secondary, this hole must be no larger than 294 mm.

The center of the secondary is not used because the rays that would have reflected off of this region are obscured by the secondary, preventing their reflection off of the primary. For all field angles, the size of the unused spot on the secondary has a diameter of 28.56 mm. As the field angle moves this spot moves but there is a central region, 13.34 mm in diameter, that is never illuminated for all field angles.

3. SENSITIVITIES

As the off-axis angle increases the WFE increases by roughly 2 μm for either a Cassegrain or a Ritchey-Chretian design. Table 4 shows the WFE as a function of the field angle for both designs.

Table 4. WFE for 3 Field Angles

	Cassegrain WFE (μm)	Ritchey-Chretian WFE (μm)
on-axis	0.05	0.19
10.6'	1.19	0.97
15'	2.32	1.91

At the full field (15'), for both designs, the major contribution to the WFE is astigmatism. For the Ritchey-Chretian design not only is coma less than for the Cassegrain design, which is expected, but so is the astigmatism. Figure 4 shows the sagittal, tangential and best focus positions in the focal plane as a function of off axis position.

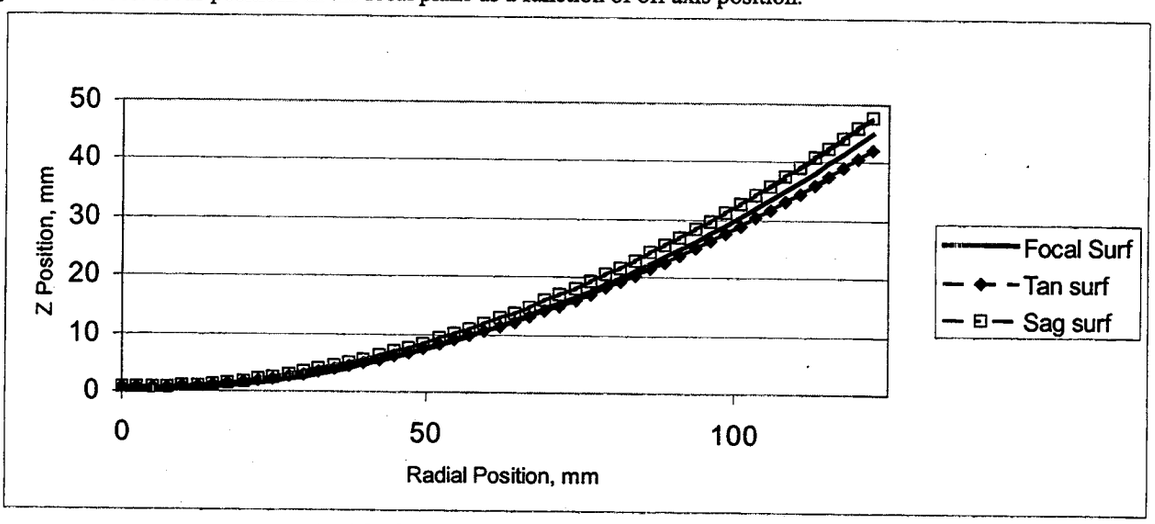

Figure 4a. Focal Surface and Surfaces with the Best Sagittal and Tangential Focus

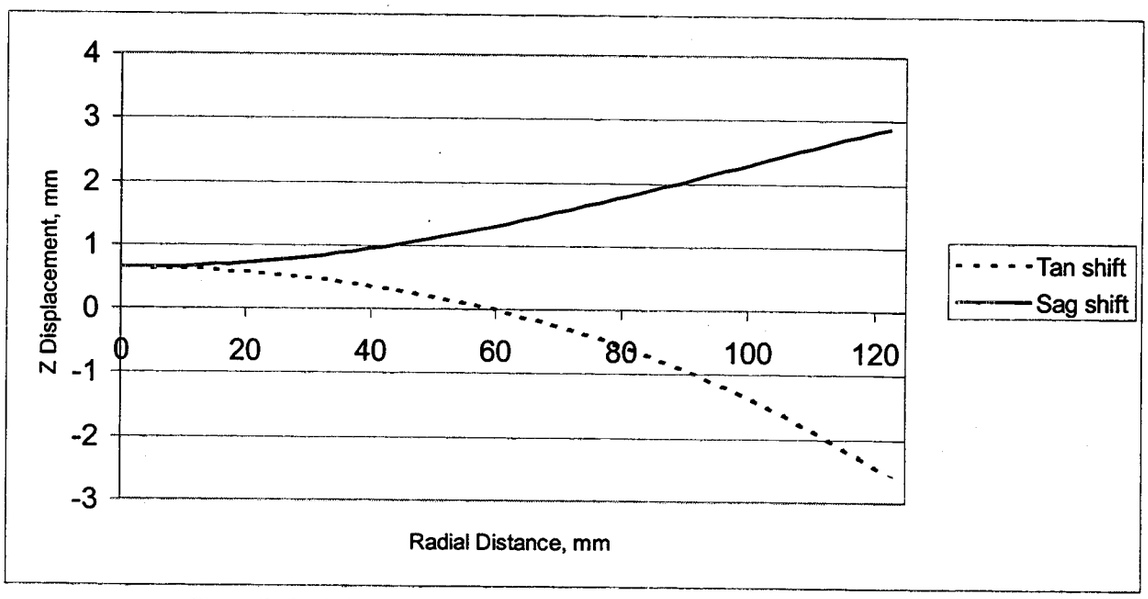

Figure 4b. Deviation of the Best Sagittal and Tangential Focus From the Focal Surface

The sensitivity of the design to various perturbations is given in table 5. Each number represents the perturbation, when applied by itself and uncompensated, that would cause a 1 μm WFE. For example a 10 μm change in the spacing between the primary and secondary would cause a 1 μm WFE.

Table 5. Perturbations That When Uncompensated Result in a 1 μm WFE

Primary mirror	ROC change	Despace secondary to primary	Decenter	Conic constant change
	19 μm	10 μm	47 μm	9.3×10^{-5}
Secondary mirror	ROC change	Despace secondary and primary to focal surface	Decenter	Conic constant change
	22 μm	2,046 μm	47 μm	1.251×10^{-3}

Most of these sensitivities show that the WFE is extremely sensitive to the various perturbations as would be expected for fast optics. The f/# of the primary is 0.5 and the f/# of the secondary is 0.561.

4. CURRENT WORK IN PROGRESS

4.1. Secondary Mirror Figure Correction

The surface error on the primary mirror will be dominated by low spatial frequency errors. Our current plan is to correct these errors by figuring the secondary as opposed to figuring the primary. At the time the secondary is manufactured, it will be figured to the shape specified in table 3. After the first low temperature measurement of the low spatial frequency errors, the secondary will be reverse figured to correct for these errors. It is believed that the largest source of error in this process is that due to the error in the measurement of the low spatial frequency errors on the primary mirror.

4.2. Stray Light

Thermal emission from the telescope is the main source of stray light. ESTEC specifies that the thermal emission from all sources, outside of that contributed by the primary and secondary mirrors, must contribute no more than 10% of that contributed by the primary and secondary mirrors combined, at a detector element. The last part of the requirement is very important because most stray light reaching the focal plane will not enter the detectors because aperture stops will be used in the instruments. Nevertheless a starting point is to consider the flux entering the focal plane and afterwards calculate the flux entering a detector element. Table 6 gives the flux entering the focal plane and the average spectral irradiance from the primary and secondary mirrors for 3 wavelength bands. For this calculation an emissivity of 0.01 was assumed for each mirror and a temperature of 80 K was assumed for the primary mirror and 70 K for the secondary mirror.

Table 6. Thermal Emission From Primary and Secondary Mirrors into Focal Surface

Bandwidth (μm)	Flux collected in focal plane (μW)	Spectral Irradiance at focal surface ($\mu W/m^2$-μm)
80 - 100	0.58	0.62
200 - 300	0.11	0.024
500 - 600	0.006	0.0013

The focal plane, for this calculation, is a circle of radius 122 mm. An estimate of the thermal emission from the struts (assuming an emissivity of 0.04 and a temperature of 75 K) for the 200 to 300 μm range is 4.2 nW or 3.8% of the emission of the primary and secondary mirrors. The struts and the hole through the primary mirror into the cryostat are expected to be the largest sources of stray light.

Tripod strut design has a large effect on the stray light and this is mostly discussed in reference 2.

4.3. Primary Mirror Gaps

The primary mirror is not made of a contiguous facesheet, but rather of 6 independent pie shaped facesheets, that are held together by a contiguous core to form a monolithic mirror. Facesheet gaps, roughly 2 mm wide, are the source of additional stray light. The diffractive effects of these gaps on stray light and imaging are still being analyzed, but it appears that the largest stray light effect is due to the gaps acting as a blackbody. This is a small effect because the gaps comprise only 0.16% of the primary mirror's area (the area from the part of 3 gaps that extends from the tripod leg fitting to the edge of the primary is not included because the radiation from this region cannot reach the focal plane). To estimate the increase in thermal

background due to the gaps assume that the temperature of the gaps is no different than the mirror (it differs by less than 0.1 K) but has an emissivity 100 times larger (assume that the emissivity of the primary is 0.01 and the emissivity of the gaps is unity). The result is an increase in the thermal emission of the primary mirror by 16%.

The following analysis was done to bound the thermal background picked up from the sunshade due to diffraction by the gaps compared to the thermal background from the primary mirror's emission. Analysis of the total diffractive effect of the gaps shows that for small gap widths compared to the mirror's diameter (which is certainly our case) the fraction of energy kicked out of the Airy disk due to the gaps is proportional to the area of the gaps divided by the area of the primary mirror (0.16%). Working the optics backwards, assuming that a beam is transmitted from the focal point of the system, 0.16% of these transmitted rays are diffracted by the gaps. The longer the wavelength the larger the diffraction angle making it more likely that longer wavelength rays than shorter wavelength rays will see the sunshade. As a result our worst case estimate will use the longest observational wavelength, 670 μm. At this wavelength roughly 50% of the rays diffracted by the gaps are diffracted at angles large enough to see the sunshade. Thus, 0.08% (0.5x0.16%) of the rays transmitted from the focal point are diffracted at angles large enough to see the sunshade. Not all of these rays see the sunshade since the sunshade surrounds only 35% of the primary mirror. Thus the efficiency of diffracting 670 μm rays from the sunshade to the focal plane, taking into account the sunshade's view factor, compared to energy emitted by the primary mirror is 0.028% (0.5x0.35x0.16%). What is left to consider is the sunshade's thermal emission relative to the primary mirror's thermal emission The sunshade is roughly 2.2 times warmer than the primary (173 K/80 K) and roughly 5 times more emissive (0.05/0.01). The final upper limit is that the contribution to the thermal background, due to gap diffraction at 670 μm, is less than 0.3% of the thermal background of the primary (2.2x5x0.028%).

4.4. Standing Wave Impact On HIFI

The HIFI is sensitive to standing waves generated between the instrument and the secondary mirror. These waves originate from internal mixer noise transmitted to the secondary which are then reflected or diffracted back to the detector. Some of the returned signal is correlated with the internal mixer noise. The correlated signals add vectorially and their amplitude depends on the phase between the signals. The phase depends on the extra path traveled by the signal that reflected off of the secondary and the frequency of the signal. As a result there is a frequency dependent ripple sitting on the noise floor.

Two paths allow for standing waves from the secondary. One path is from the center of the secondary (narcissus effect) and the other is diffraction off of the edge of the secondary. To mitigate the former effect a spoiler will be placed on the center of the secondary to reflect the mixer noise to cold space (after one reflection off of the primary). The latter effect is reduced by having a varying return path from the edge of the secondary so that the diffracted energy from this edge cannot be in phase when it returns to the focal plane. The power in the reflected signal must be reduced by 92 dB at all wavelengths. Without installing a spoiler the power rejection, for the signal off of the center of the secondary, varies from 50 dB for channel 1 frequencies (480 - 642 GHz) to 65 dB for channel 7 frequencies (2400 - 2700 GHz).

ACKNOWLEDGMENTS

The work described in this paper was carried out by the Jet Propulsion Laboratory, California Institute of Technology, under a contract with the National Aeronautics and Space Administration. The following people at JPL have supported the work in this paper; Tom Borden with discussions on the FIRST program and in assembling the paper, Andrew Lowman with the gap diffraction analysis, and Larry Scherr for stray light analysis. Dustin Crumb, of Swales Aerospace produced the picture of FIRST.

REFERENCES

1. G. L. Pilbratt, "FIRST ESA conerstone mission", *UV, Optical, and IR Space Telescopes and Instruments*, editors J. B. Breckinridge and P. Jakobsen, SPIE conference 4013, Munich, 2000.
2. E. J. Cohen, S. J. Connell, K. J. Dodson, J. L. Abbott, A. A. Abusafieh, Z. F. Backovsky, J. E. Dyer, J. Escobedo-Torres, Z. Friedman, A. B. Hull, D. W. Small, P. Thorndyke, and S. A. Whitmore, "Architecture of the FIRST telescope", *Radio Telescopes*, editor H. R. Butcher, SPIE conference 4015, Munich, 2000.
3. T. de Graauw, et. al., "Heterodyne instrument for FIRST (HIFI): design and development status", *UV, Optical, and IR Space Telescopes and Instruments*, editors J. B. Breckinridge and P. Jakobsen, SPIE conference 4013, Munich, 2000.
4. A. Poglitsch, N. Geis, and C. Waelkens, "Photoconductor array camera and spectrometer (PACS) for FIRST", *UV, Optical, and IR Space Telescopes and Instruments*, editors J. B. Breckinridge and P. Jakobsen, SPIE conference 4013, Munich, 2000.
5. M. J. Griffin, B. M. Swinyard, L. G.Vigroux, "SPIRE instrument for FIRST", *UV, Optical, and IR Space Telescopes and Instruments*, editors J. B. Breckinridge and P. Jakobsen, SPIE conference 4013, Munich, 2000.